ACS APPLIED MATERIALS & INTERFACES

Forum Article

www.acsami.org

Quantum Dot-Based, Quantitative, and Multiplexed Assay for Tissue Staining

Hong Xu,[†] Jing Xu,[‡,§] Xu Wang,[‡] Daqing Wu,[‡] Zhuo Georgia Chen,[‡] and Andrew Y. Wang*[,†]

[†]Ocean NanoTech, LLC, Springdale, Arkansas 72764, United States

[‡]Winship Cancer Institute, Emory University, Atlanta, Georgia 30322, United States

[§]Xiang Ya School of Medicine, Central South University, Changsha, Hunan, China

ABSTRACT: The excellent optical properties of quantum dots (QDs), such as high brightness, high photostability, continuous absorption, and narrow emission bandwidth, make them ideal as optical labels to develop QD-based immunohistofluorescence (IHF) imaging for multiplexing cancer biomarker detection on formalin-fixed and paraffin-embedded (FFPE) tissues. IHF is very important for the prediction of a patient's response to cancer chemotherapy or radiotherapy. QD-based IHF faces several challenges that differ from those encountered by organic dye based IHF for clinical assays. The current work addresses some of these issues. Initially, the chemical stability of QDs and organic dyes were compared. The results showed that QDs were stable for at least 5 months on FFPE tissue, whereas organic dyes were photobleached shortly after exposure to light. Various staining methods were also studied. QD fluorescence intensity on the tissue stained with primary antibody (Ab, p16, survivin, EF1α) conjugated QDs from our company was comparable to the signal from a commercially available method in which the tissue was stained with a primary p16 Ab and a QD-labeled secondary goat anti mouse Ab respectively. Finally, the effect of the amount of Ab conjugated to QD on tissue imaging was also studied. There was no significant increase in the QD fluorescence signal on tissues when the Ab:QD ratio increased from 5 to 30. In addition, protein G was tested as an adaptor protein to link Ab to QDs for IHF staining. However, the proper blocking of the protein G on QDs was necessary to reduce crosstalk. The biomarker quantification in QD-based IHF was validated by conventional Western blot and immunohistochemistry. The results contained herein demonstrate a promising application of QDs in multiplex detection and quantification of biomarkers.

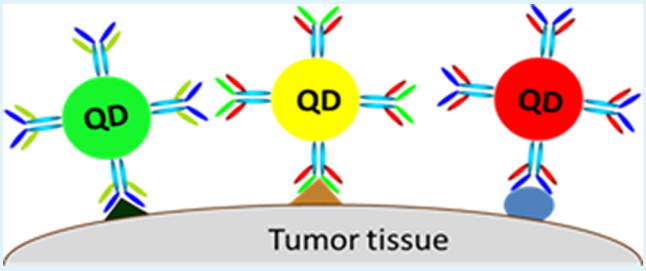

KEYWORDS: *quantum dots, targeted tissue imaging, multiplexing, cancer biomarker detection, biomarker quantification*

INTRODUCTION

There is a need for novel technology that can simultaneously detect multiple cancer molecular markers on cancerous tissues. Such technology must also have the capability to correlate with traditional pathology and histology screening methods for early cancer detection and with evaluations used to predict a patient's response to therapy.[1−3] With new molecular profiling technologies, such as RT-PCR, gene chips, protein chips, two-dimensional gel electrophoresis, and biomolecular mass spectrometry (LC-MS, etc.), it is possible to read the molecular signatures of an individual patient's tumor and to correlate a panel of biomarkers with clinical outcomes to better determine personalized therapy. However, most tumors are highly heterogeneous; containing a mixture of benign, cancerous, and stroma cells. The heterogeneous nature of tumors makes it difficult to use the aforementioned technologies for precise molecular profiling. Furthermore, a common limitation of these technologies is that they require digestion of cells or tissue specimens into a homogeneous solution, leading to a loss of valuable cellular and tissue morphological information associated with the original tumor, as well as a loss in bioactivity of biomolecules that require a tissue environment.

Biomolecules—including antigen-specific antibodies (Abs)—with a high-affinity for tumor-associated biomarkers have been used to detect solid tumors and tumor-associated vasculature in animal models as well as in clinical trials patients using tissue imaging techniques.[4−8] Well-established techniques for tissue imaging include immunohistochemistry (IHC) and immunohistofluorescence (IHF). These highly precise approaches are capable of providing molecular information down to the level of a single cell. They also provide the ability to look at different cell populations simultaneously. This feature provides assurance that the molecular signature being studied actually arises in the cells of interest, while also taking into account "field effects," which are areas in which anatomically normal tissues that are adjacent to abnormal regions exhibit molecular abnormalities. However, signal-to-background ratio

Special Issue: Forum on Biomedical Applications of Colloidal Photoluminescent Quantum Dots

Received: December 27, 2012
Accepted: March 20, 2013
Published: April 3, 2013

may not be large enough to be quantified when one looks at individual cells vs population extracts because even one cell among millions can be detected and studied. Furthermore, IHC coupled with conventional imaging techniques is not well suited for quantification of more than two or three biomarkers at a time for optical reasons. The current solution for multiplexed biomarker detection is either the serial-section approach, or immunofluorescence. Serial sections are sequential micro slices of a paraffin block that are stained individually for different antigens. Typically, a cell present in one "slice" may not always be present on the next section.

Fluorescence is better suited than IHC for multiplexing multiple signals on a single tissue section. It has a higher dynamic range than bright-field chromogenic staining techniques, but also suffers from several drawbacks. Fluorescence signals can often be photobleached, causing them to disappear. Also, tissue autofluorescence—a major problem with formalin-fixed and paraffin-embedded (FFPE) tissue specimen samples—can partially or completely obscure signals in the visible light range, therefore limiting multiplexing options.[6−11] Spectral imaging can enhance the multiplexing capabilities of IHF and can largely eliminate problems due to autofluorescence, greatly improving sensitivity. Thus, if true multiplexing were possible using IHF, IHC, or IHC and IHF combined on a single sample, the goal of precisely resolved single-cell multibiomarker phenotyping could be achieved using spectral imaging. The recent development of fluorescent quantum dots (QDs) has greatly enhanced the possibility to achieve this goal using IHF. With novel optical properties such as high brightness, high photostability, continuous absorption, and narrow emission bandwidth,[12−18] QD-based IHF is ideal for multiplex biomarker detection on tissue specimens, which are well documented in many publications for past several years.[19−25] To fully utilize the advantage of the QDs for multiplexing imaging and to translate the QDs to clinic application, here, we address several factors of QDs for multiplexing tissue biomarkers including development of protein G as universal adaptor to form antibody-QD conjugates that potentially avoid chemical treatment of the antibody and control orientation of the antibody on QD surface to increase the bioaffinity; Stability, specificity and sensitivity testing of QD-based multiplex staining on FFPE tissues; optimization of the ratio of the antibodies on the QDs for tissue staining; staining methods and quantification method. In combination with a multispectral imaging system, results from the QD-based IHF were then compared to those obtained from conventional Western blot analysis and IHC.

METHODS AND MATERIALS

Cell Cultures and Tissue Preparation. Both CaSki and U937 were purchased from American Type Culture Collection (Manassas, VA). CaSki is a cervical cancer cell line which contains the genome of human papillomavirus 16. U937 is macrophage cell line obtained from the pleural effusion of a patient with histiocytic lymphoma. CaSki and U937 cells were cultured in PRMI1640 supplemented with 10% FBS (fetal bovine serum) at 37 °C with 5% CO_2. Human head and neck cancer cell line SCC090 was cultured in DMEM/F12 supplemented with 10% FBS at 37 °C with 5% CO_2. FFPE tissue slides of head and neck cancer were obtained from Emory University Hospital and their usage was approved by the Institutional Review Board with a HIPPA compliance.

QD−Protein Conjugation. Carboxylic acid-functionalized QDs (QSH, Ocean NanoTech) with emission peaks at 529, 546, 573, and 623 nm were used for the preparation of QD-Ab conjugated, which optical properties and size were listed in Table 1. 1-Ethyl-3-[3-dimethylaminopropyl]carbodiimide hydrochloride (EDC) coupling method was used to conjugate antibody to QDs directly. Briefly, 1 nmole of carboxyl functionalized QD (QSH, Ocean Nanotech, LLC, Springdale, AR) in 425 uL of 10 mM borate buffer (pH 7.4) and 2 nmoles of Abs (p16, survivin, EF1α, or otherwise indicated) or 20 nmoles of protein G were mixed together. Then, 0.2 mg EDC was added and the reaction mixture was incubated on a shaker at room temperature (RT). After 30 min, the reaction progress was checked by gel electrophoresis to see if the QSH was attached to the protein. The reaction was quenched with 5 mg/mL monoamine polyethyl glycol (PEG) 2000 after 1 h. The QD-protein conjugates were purified and washed twice with borate buffer (20 mM, pH 7.0) by ultra-centrifugation. Anti survivin (Lifespan BioSciences, Seattle, WA), anti EF1α (EMD Millipore, Billerica, MA), goat anti mouse IgG (Jackson ImmunoResearch, West Grove, PA), anti p16 (Santa Cruz Biotechnology, Inc., CA), and anti β-actin (Santa Cruz Biotechnology, Inc., CA) were conjugated to QDs.

Primary Abs were loaded onto the QD−protein G (PG) surface at 2:1 ratio by incubating the Ab and the QD together at RT for 1 h, followed by incubation with 2% bovine serum albumin (BSA) for additional 1 h to block the unused sites on protein G.

Table 1. Characterization of Carboxyl-Terminated QDs (Ocean Nanotech cat # QSH) Used in This Study

catalog number	absorption peak (nm)	emission peak (nm)	quantum yield (%)	fwhm (nm)[a]	hydrodynamic size (nm)[b]
QSH620	611	623	60	25	12.7 ± 2.2
QSH573	558	573	50	26	12.4 ± 0.4
QSH550	527	546	50	30	10.7 ± 2.2
QSH530	514	529	40	30	10.2 ± 1.9

[a]fwhm: full width half-maximum. [b]Hydrodynamic size was measured by Zetatrac (Microtrac, Inc., PA, USA).

Construction of HPV16E6 Negative Cells. To obtain HPV negative cells, the HPV16E6 specific shRNA lentivirus to silence HPV16E6 or the control shRNA lentivirus (Santa Cruz Biotechnology, Inc., CA) were used for the transfection of HPV positive cells following the protocol provided by the manufacturer. Briefly, HPV positive CaSki cells were seeded into a 12-well plate at the density of 5000 cells per well 24 h prior to the viral transfection. Lentiviral particles were thawed at room temperature (RT) and diluted 10 times with complete medium supplemented with 5 μg/mL of polybrene. Cells were incubated in the medium containing lentivurus for 12 h and then fresh complete medium (without Polybrene) for 2 more days. Stable puromycin resistant CaSki cells were selected by continuous culturing of cells in medium supplemented with 2 μg/mL puromycin for 2 weeks or until single colonies appeared.

Western Blot. Cells were harvested and lyzed in lysis buffer (50 mM Tris-HCl, pH 8.1, 1% SDS) to extract the total protein. The concentration of protein was determined by via the BCA protein quantification method. Total protein (80 μg) was separated by 12% SDS-PAGE and then transferred onto a nitrocellulose membrane. The membrane was blocked with 5% albumin in TBST (20 mM Tris-HCl, pH 8.0, 150 mM NaCl, 0.1% Tween-20) for 1 h at RT and then incubated with primary antibodies overnight at 4 °C. Anti p16 Ab (1:1000 dilution, clone C-20, Santa Cruz Biotechnology, Inc., CA), anti HPV16E6 Ab (1:1000 dilution, clone N17, Santa Cruz Biotechnology, Inc., CA), and anti β-actin Ab (1:1000 dilution, Santa Cruz Biotechnology, Inc., CA) were used for these studies. The membrane containing the transferred proteins was washed three times with TBST and incubated with secondary antibody (1:5000 dilution) for one hour at RT. Secondary antibody binding signals were captured on film after using enhanced chemiluminescence detection reagent (Amersham Pharmacia Biotech, Inc., Piscataway, NJ). After the images were scanned to a computer, ImageJ software was used to quantify the intensity of the antibody binding signals.

IHC Staining of FFPE Tissues. FFPE slides were stained with the CINtec HISTOLOGY kit for p16 using the DAKO Autostainer (Dako North America, Inc., Carpinteria, CA).

Labeling of U937 Cells. U937 cells in suspension were harvested by centrifugation (500g × 5 min) and washed three times with 1 mL phosphate-buffered saline (PBS). The cocktail of QD-Ab conjugates was incubated with cells for 20 min at RT, after which the cells were washed three times with rinsing buffer RBB (Ocean Nanotech, LLC., Springdale, AR) and then with PBS. Following mounting on microscope slides, the cells were observed under fluorescent microscope (Amscope MD800E) and pictures were taken using Amscope image software.

Labeling of Cancer Cells. Cancer cells (1×10^4) were seeded into an 8-well plate with glass coverslips per well. The cells were fixed with 4% paraformaldehyde, permeabilized with 0.25% TritonX 100 in PBS for 30 min at RT, blocked with 2.5% horse serum for 30 min, and incubated with an appropriate dilution of the primary Abs overnight at 4 °C. Cells were exposed to QD−secondary Abs for 1 h at 37 °C after washing with PBS. For staining with QD-primary Ab conjugates, cells were exposed to QD-primary Ab for 1 h at RT. Cell nuclei were counterstained by using 4, 6-diamidino-2-phenylindole (DAPI).

Labeling of Clinical Tumor Tissues. Archived FFPE tissue blocks were obtained from banked tissues collected as part of routine surgical interventions with consent from Tissue Procurement Service at Emory School of Medicine, an IRB-approved Tissue Procurement and Banking Facility Core. The cases were selected from oropharyngeal squamous cell carcinomas (OPSCC), which have high incidence of HPV16 infection. We selected 3 of each p16-positive and -negative OPSCC tissues for this study since p16 is a surrogate biomarker for HPV16. The primary goal for this study is to validate QD-p16 antibody conjugate; therefore, additional clinical information for these tissues was not provided. Staining of FFPE tissues followed the standard protocol. In brief, after deparaffinization with xylene and rehydration with ethanol, endogenous peroxidase activity was blocked by incubating the slides in 3% hydrogen peroxide with methanol for 15 min. To retrieve the antigens, the tissue slides were heated in a microwave oven in 100 mM sodium citrate buffer (pH 6.0) for 15 min and then allowed to remain at RT for 20 min. After washing with PBS, the slides were incubated with 2.5% normal horse serum for 20 min to decrease the background signal. The slides were then incubated with an appropriate dilution of the primary Abs overnight at 4 °C. Cells were exposed to QD−secondary Abs for 1 h at 37 °C after washing with PBS. For staining with QD−primary Ab conjugates, cells were exposed to QD−primary Ab for 1 h at RT. Cell nuclei were counterstained using DAPI.

Multispectral Imaging and Signal Quantification. After staining the cells and tissue specifically with the respective QD-Ab conjugates, the CRI Nuance spectral imaging and quantifying system (Caliper Life Science, Waltham, MA) was used to observe and quantify the QD signal. Ten cubed images from 10 randomly selected areas were collected from each cell slide at 10-nm wavelength sections between 500 to 800 nm, with an auto exposure time per wavelength interval at 100× or 400× magnification.

Taking the cube with a long wavelength bypass filter allowed transmission of all emission wavelengths above 450 nm. Both separated and combined QD images were established after determining the QD spectral library and segregating the cube. For accurate quantification of the QD signals, the background was removed by assigning the autofluorescence as black color.

Using the software integrated with the CRI image system, the fluorescent signal intensity was quantified for each stained slide. After the images were taken and segregated according to the established library, either one or multiple area(s) of interest (AOI) were selected and the signal intensity for each AOI was provided by the software. The signal arbitrary unit (a.u.) is defined as the average fluorescence signal intensity per exposure time (ms), which is obtained from the Nuance software. The QD signal intensity for each sample was determined as an average a.u. (a.u.) from at least 500 selected cells.

RESULTS AND DISCUSSIONS

Photostability of QDs on Tissue and Resolution of QD-Based Staining Analyzed by Multispectral Technology.

The photostability of QD−Ab was evaluated after they were used to label FFPE tissue samples. FFPE tissues were stained with QD620−anti survivin and images were captured at time zero, 2 weeks, and 5 months after the staining. Survivin is selectively expressed in most human cancers but is undetectable in most healthy adult tissues.

As shown in Figure 1A, cancerous tissue was heavily stained with QD620-anti survivin Ab, while the surrounding tissue was

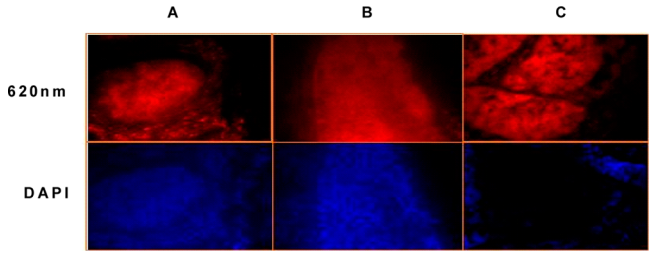

Figure 1. Photostability of QD on tissues. FFPE tissues were stained with QD620-anti survivin. Images were captured using CRI to generate intensity dependent images from 620 nm and DAPI channels (A) immediately, (B) 2 weeks, and (C) 5 months after staining.

only lightly stained. The signals from QD and DAPI were still very stable after 2 weeks (Figure 1B). After the tissues with QDs and DAPI staining were stored under dark for 5 months, images were taken again to check the stability of QD−Ab conjugates by comparison with their emission. The QD-Ab attached to cancerous tissue still showed a very bright fluorescent color (Figure 1C). The DAPI dye mostly faded away after 5 months. Because QDs are made from inorganic semiconductors, they tend to have higher chemical stability than organic dyes, which are susceptible to oxidation when exposed to the air. The high chemical stability of QDs, which related to their photostability, is highly favorable for many applications.

Figure 2 demonstrates the resolution of the QD-based multiplex staining system. The tissue slide was stained with

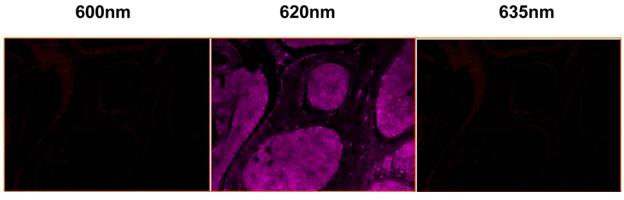

Figure 2. Resolution of QD-based IHF. FFPE tissues were stained with QD620-anti surviving and DAPI. Images were captured using CRI to generate intensity dependent images from 600, 620, and 635 nm channels. Signals from 620 nm channel were more than 1000 times stronger than those from 600 and 635 nm channels, indicating the narrow emission bandwidth of QDs.

QD620-anti survivin Ab and analyzed with QD600, QD620, and QD635 as fluorescent stain set in a signal library. After the image was simplified, signals obtained from the image were quantified. The signal from the 620 nm channel was over 1000 times stronger than that from the 635 and 600 nm channels. This indicates that the QDs had a very narrow emission bandwidth and that the imaging system was able to identify the difference between two QDs whose maximum emission wavelengths were only 15 nm apart. The sharp emission peak and size tunable property of QDs allows for a number of

choices for the emission color of the QDs. Therefore, QDs are able to be used for multiplex staining in the visible light range.

Comparison of Different Staining Methods. The current approach for cell or tissue labeling employs either secondary Ab-conjugated QDs to target primary Ab, or direct conjugation between primary Ab and QDs. We carried out the comparison of FFPE tissues stained with QD−secondary Ab or QD−primary Ab. Two FFPE tissue slides from the same patient were stained with QD573-anti p16 or anti p16/QD573-secondary Ab and the signals were quantified. p16 is an important regulator in the cell cycle and its overexpression was found to be significantly correlated with HPV-associated head and neck cancer and carcinogenic processes.[14,15] As shown in Figure 3A, consistently in the three independent assays, the

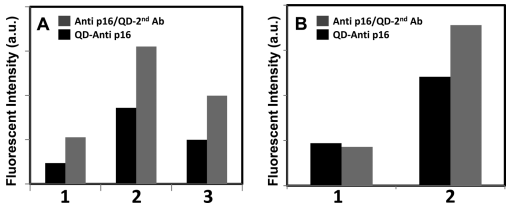

Figure 3. Comparison of immune-staining signals using QD-primary Ab and QD−secondary Ab. (A) Two FFPE tissue slides from the same patient (#1, #2, and #3) were stained with QD573-anti p16 or anti p16/QD573-secondary Ab. (B) FFPE tissue slides from p16 negative (1) or p16 positive (2) patients (verified by IHC) were stained with QD573−anti p16 or anti p16/QD573−secondary Ab. Signal intensity of QD573 was quantified using the software integrated with CRI system.

signals from two different staining methods were similar; although immuno-staining using the QD-secondary Ab gave a stronger immunofluorescence signal than that using the QD-primary Ab. We further compared immuno-staining using first-Ab-QD and second-Ab-QD by looking for the larger difference between p16 positive and negative samples (verified by IHC) instead of brighter signals. In each staining group, three p16 positive and three p16 negative slides were used and the average signals were presented in Figure 3B. The difference between positive and negative slides was slightly larger using anti-p16/2nd-Ab-QD staining than with the anti-p16-Ab-QD staining (3.75 fold vs. 2.75 fold).

The secondary Ab−QD approach is limited by choices for primary antibodies, which have to be raised from different species, for multiplexing to avoid cross-binding when the secondary antibody−QDs are applied. Not all primary antibodies have an ideal isotype available. The direct QD−primary Ab conjugation method would avoid the species matching problem. However, the use of primary antibodies is a risky endeavor because of the high cost of primary Abs.

Direct QD conjugation methods may suffer from several major problems, which limit their application in cancer molecular profiling. First, antibodies are linked to QDs via chemical reactions. The type of chemical reactions required are harsh and can reduce antibody binding affinity and activity. Second, the Ab's orientation on the QD surface is uncontrollable. Because the F(ab)2 domain of an Ab is responsible for specific target recognition, exposing Fc domain not only loses the bioaffinity toward its antigen but may also introduce nonspecific adsorption or uptake both in vitro and in vivo.

In addition to direct conjugation, another possible conjugation approach is using protein G (pG) as an adaptor to attach Ab to the QD surface. This method is easy to prepare and allows for correct antibody orientation.[26−28] However, it is possible that Abs captured on pG can migrate and interchange because the pG∼Ab bond is labile. To examine this phenomenon, we compared the staining effect of QD-pG∼Ab with that of QD-Ab using the macrophage cell line U937 in suspension. This cell line does not have the survivin biomarker, but instead expresses the housekeeping protein elongation factor 1α (EF1α). Thus, it is expected that the U937 cell will not be stained with the QD620-pG∼anti survivin (red) or the QD620-anti survivin (red) Abs but will be stained with the QD530-pG∼anti EF1α (green) or the QD530-anti EF1α (green).

The results in Figure 4B show that when QD620-pG∼anti survivin and QD530-pG∼anti EF1α Abs were used, the QD620

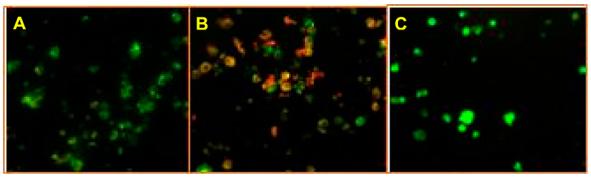

Figure 4. Cross-migration of Ab attached to protein G. Using U937 cells that do not contain the biomarker survivin, (B) cross-migration of antisurvivin that was immobilized on QD−PG−Ab was observed as red signals mixed with green signals in the absence of survivin. (A) The mixed signal was not observed in QD−Abs. (C) After blocking the pG binding sites on QD∼pG before cell staining, the mixed signal was no longer observed.

signal was observed even in the absence of the biomarker survivin in U937 cells. On the other hand, when QD620-anti survivin and QD530-anti EF1α were used, the red signal from QD-anti survivin was not observed (Figure 4A). Thus, cross migration of Abs did happen on protein G. To avoid antibody exchange in QD-pG∼Ab, we blocked the unused sites on the protein G using 2% BSA before cell staining. The red signal was not observed after staining cells with the blocked QD-pG∼Abs (Figure 4C).

Optimization of QD-Based Staining Signals by Varying Ab to QD Ratios. To study the effects of different QD to Ab ratio on the intensity of the IHF signal, we chose to conjugate QD with different ratios of a secondary Ab goat antimouse IgG and use these conjugates to stain cancer cells. Labeling secondary Abs is currently popular among commercially available immunofluorescence staining products.

Goat antimouse IgG was first conjugated with QSH550 at different ratios (2:1, 5:1, 10:1, 20:1, or 30:1) to form QD550−Ab. SCC090 cells were stained with anti p16 (mouse anti human) and then QD550-Abs which have different amounts of secondary Ab (goat anti mouse) on the surface. After being costained with nuclei specific DAPI, a total of 500 cells were randomly selected from 10 images for the quantification.

As shown in Figure 5, there was no substantial difference in IHF signals at the various ratios tested using the QD550−secondary Ab. The Ab ratio of 1:20 showed a stronger immuno-fluorescent signal than the QD−secondary Ab molar ratio of 1:10 or less. Considering the cost of Abs, the QD to Ab ratio of 1:5 was more cost efficient (even with an insignificant loss in staining signal) than the other ratios.

Comparison of QD-Based IHF with Conventional Western Blot and IHC. Quantification of biomarkers is the ultimate goal of this QD-based IHF method. To use the QD-

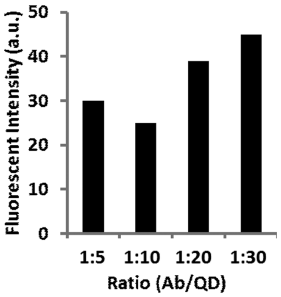

Figure 5. Effects of QD to antibody ratios on the staining signal intensity. Human cervical cancer CaSki cells were first stained with anti p16 (mouse anti human) and then QD550, which have different amounts of secondary Ab (goat anti mouse IgG) on the surface (1:5, 1:10, 1:20, and 1:30) to recognize the primary Ab. Signal intensity of QD550 was quantified from the average of 10 randomly selected images using CRi InForm software.

based multiplex staining technology for in vitro diagnostics, we first need to validate the quantification of biomarkers by QD-based staining by comparing this method with conventional Western blot and IHC methods.

Initially, we quantified signals from the QD-based staining of cells and compared the results to those obtained from Western blot analysis. Using anti-p16−∼QD573, we compared the staining results of a HPV16E6 knockdown (mutated via shRNA lentivirus transfection, validation as in Figure 6I) with that of the wild type ($HPV16^+$) CaSki cells. Our results show that both anti-p16−QD573 Ab staining and the Western blot analysis were able to detect the restoration of p16 protein in the E6 knockdown cells (Figure 6C, G). This result is consistent with previous publications.[14,15] On the basis of the notion that the expression level of β-actin is relatively constant in different cells and tissues, the slides were costained with the QD conjugated with anti-β-actin as an internal control for normalization of the signal intensity from different batches of QD and/or FFPE tissue slide preparations. Comparison of quantification results between QD-based multiplex staining and Western blot analysis was also carried out (Figure 6I, J). Both quantification methods indicated the restoration of p16 in HPV16 E6 knockdown cells was successful.

Staining of p16 on FFPE tissues was performed by QD-based IHF and compared with the conventional IHC method. The tissue slides were stained by QD-labeled anti p16 antibody with the same clone number using the identical conditions as used in the IHC. Our study showed that similar to the IHC method, QD−IHF could clearly distinguish positive and negative p16 samples (Figure 7).

Multiplex Staining of FFPE Tissue Samples. The biomarker survivin and the internal control EF1α were stained simultaneously on FFPE tissue slides using QD−primary Ab conjugates. Cell nuclei specific DAPI staining on the same slide was used to identify cells during imaging. Because of different expression levels of proteins and different brightness for each QD, EF1α (a house keeping protein) was assigned to QD530 (weak fluorescence emission) and survivin was assigned to QD620 (strong fluorescence emission). As shown in Figure 8, QD620 signals were present only in the cancerous tissues as indicated by the large nuclei stained by DAPI, whereas EF1α was present in both cancerous and surrounding tissues.

Quantification of Signals from Multiplex Stained Cells and Tissues. Signals from the different channels and different tissue types were quantified on a multiplex stained FFPE slide (Table 2). The survivin expression level was much higher than that of EF1α in the cancerous tissue, whereas the expression

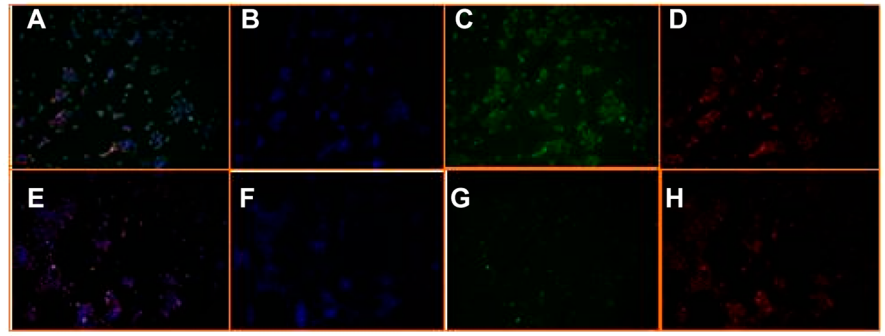

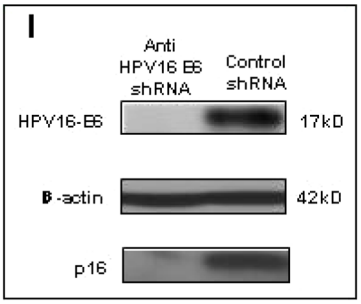

J

	Western blot analysis		QD-based staining	
	Wild-type cells (HPV^+)	Knockdown cells (HPV^-)	Wild-type cells (HPV^+)	Knockdown cells (HPV^-)
p16	13	4	42	32
β-actin	63	62	49	60
P16/ β-actin	0.21	0.06	0.86	0.53

Figure 6. Comparison of QD-based staining with Western blot analysis for p16 detection. (A−D) HPV16-E6 knockdown or (E−H) wild-type CaSki cells were multiplex stained with (D, H) QD550−anti β-actin, (C, G) QD573−anti-p16, and (B, F) nuclear specific dye DAPI. Images were captured using CRI multispectral imaging system to generate intensity-dependent images from each of the three color channels. (A, E) Merged images are also presented. Total protein was extracted from these two strains of CaSki cell lines. HPV16 E6, p16, and β-actin were detected by (I) Western blot analysis. (J) Expression levels of β-actin and p16 were quantified as illustrated as arbitrary unit on westen blot analysis and QD-based IHF by densitometer and CRi imaging system, respectively.

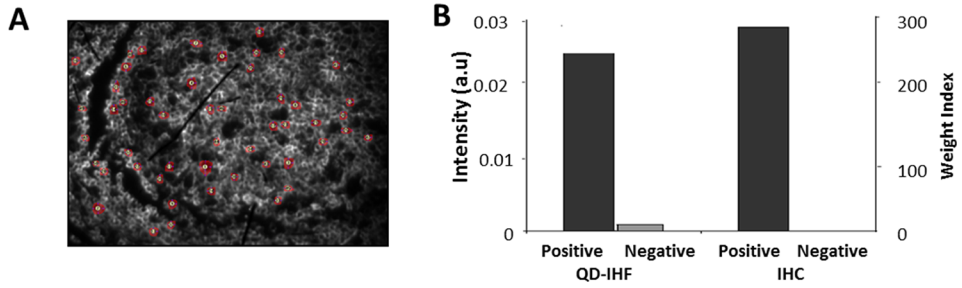

Figure 7. Quantification of p16 staining by QD−IHF and its comparison with conventional IHC. (A) Random selection of cancer cells (n = 50 for each image cube) for quantification of QD−-IHF signals based on cytokeratin and nuclear markers. The arbitrary unit (a.u.) of the QD−IHF signal intensity for each of the samples was obtained from an average of 10 images acquired from each sample. (B) Comparison of the signals between QD−IHF and conventional IHC in three individual HNSCC tissues.

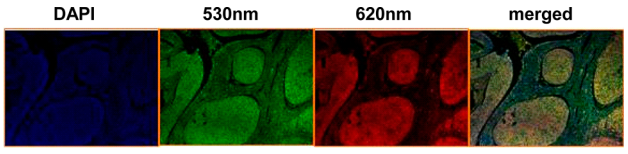

Figure 8. Multiplex staining of FFPE tissues with QD-Ab conjugates. The FFPE tissue was multiplex stained with QD530-anti EF1α, QD620-anti surviving, and the nuclear specific dye DAPI. Images were captured using CRI to generate intensity dependent images from each of the three color channels. The autofluorescence from FFPE tissues was removed by assigning it to black. The merged image is a composite image of each color. The pseudo color assignments for the merged image are as follows: DAPI, blue; QD520, green; QD620, magenta.

Table 2. Quantification of Immune-Staining Signals from QD-Based IHF[a]

tissue type	detection channel	total signal (a.u./ms)
cancerous tissue	620 nm	3163.08
	530 nm	1153.56
	autofluorescence	381.87
surrounding tissue	620 nm	43.67
	530 nm	34.91
	autofluorescence	20.74

[a]FFPE tissue was multiplex stained with QD530-anti EF1α, QD620-anti survivin, and the nuclear specific dye DAPI. Signals from 620 nm, 530 nm, and autofluorescence channels were quantified with the software integrated with CRI camera.

levels of these two proteins were not much different in the surrounding tissue.

CONCLUSION

Because of their unique optical properties, biocompatible QDs composed of nanomaterial were employed for the simultaneous detection and quantification of multiple biomarkers; which would be important for cancer diagnosis. After optimization of QD-based IHF staining and validation of the quantification results by conventional Western blot and IHC, we successfully demonstrated the promising application of QDs in multiplex detection and quantification of biomarkers. Development of a QD-based IHF system for research and clinical applications is currently an ongoing project in our research pool.

AUTHOR INFORMATION

Corresponding Author

*Phone: 1-479-751-5500. Fax: 1-479-751-5502. E-mail: awang@oceannanotech.com.

Notes

The authors declare no competing financial interest.

ACKNOWLEDGMENTS

This research was supported by the following NIH Grants: HHSN261201000125C, N44CO27031-82, R44RR028019, R43CA141870, and R33CA161873.

REFERENCES

(1) Ryerson, A. B.; Peters, E. S.; Coughlin, S. S.; Chen, V. W.; Gillison, M. L.; Reichman, M. E.; Wu, X.; Chaturvedi, A. K.; Kawaoka, K. *Cancer* **2008**, *113*, 2901−2909.
(2) *National Cancer Institute State of the Science Meeting: Squamous Cell Head and Neck Cancer and the Human Papillomavirus*; Washington, D.C., Nov 9−10, 2008 ; National Cancer Institute: Bethesda, MD, 2008.
(3) Chaturvedi, A. K.; Engels, E. A.; Anderson, W. F.; Gillison, M. L. *J. Clin. Oncol.* **2008**, *26*, 612−619.
(4) Sturgis, E. M.; Cinciripini, P. M. *Cancer* **2007**, *110*, 1429−1435.
(5) Cuschieri, K.; Wentzensen, N. *Cancer Epidemiol. Biomarkers Prev.* **2008**, *17*, 2536−2545.
(6) Levenson, R. M.; Mansfield, J. R. *Cytometry A* **2006**, *69*, 748−758.
(7) Mansfield, J. R.; Gossage, K. W.; Hoyt, C. C.; Levenson, R. M. *J. Biomed. Optics* **2005**, *10*, 41207.
(8) Clancy, B.; Cauller, L. J. *J. Neurosci. Methods* **1998**, *83*, 97−102.
(9) Baschong, W.; Suetterlin, R.; Laeng, R. H. *J. Histochem. Cytochem.* **2001**, *49*, 1565−1572.
(10) Staughton, T. J.; McGillicuddy, C. J.; Weinberg, P. D. *J. Microsc.* **2001**, *201*, 70−76.
(11) Neumann, M.; Gabel, D. *J. Histochem. Cytochem.* **2002**, *50*, 437−439.
(12) Bruchez, M., Jr.; Moronne, M.; Gin, P.; Weiss, S.; Alivisatos, A. P. *Science* **1998**, *281*, 2013−2016.
(13) Smith, A. M.; Gao, X.; Nie, S. *Photochem. Photobiol.* **2004**, *80*, 377−385.
(14) Weinberger, P. M.; Yu, Z.; Haffty, B. G.; Kowalski, D.; Harigopal, M.; Brandsma, J.; Sasaki, C.; Joe, J.; Camp, R. L.; Rimm, D. L.; Psyrri, A. *J. Clin. Oncol.* **2006**, *24*, 736−747.
(15) Lassen, P.; Eriksen, J. G.; Hamilton-Dutoit, S.; Tramm, T.; Alsner, J.; Overgaard, J. *J. Clin Oncol* **2009**, *27* (12), 1992−1998.
(16) Whaley, S. R.; English, D. S.; Hu, E. L.; Barbara, P. F.; Belcher, A. M. *Nature* **2000**, *405*, 665−668.
(17) Chan, W. C.; Nie, S. *Science* **1998**, *281*, 2016−2018.
(18) Han, M.; Gao, X.; Su, J. Z.; Nie, S. *Nat. Biotechnol.* **2001**, *19*, 631−635.

(19) Yezhelyev, M. V.; Al-Hajj, M.; Morris, C.; Marcus, A.; Liu, T.; Lewis, M.; Cohen, C.; Zrazhevskiy, P.; Simons, J. W.; Rogatko, A.; Nie, S.; Gao, X.; O'Regan, R. *Adv. Mater.* **2007**, *19* (20), 3146−3146.
(20) Huang, D. H.; Su, L.; Peng, X. H.; Zhang, H.; Khuri, F. R.; Shin, D. M.; Chen, Z. G. *Nanotechnology* **2009**, *20* (22), 225102.
(21) Xu, J.; Muller, S.; Nannapaneni, S.; Pan, L.; Wang, Y.; Peng, X.; Wang, D.; Tighiouart, M.; Chen, Z.; Saba, N. F.; Beitler, J. J.; Shin, D. M.; Chen, Z. G. *Eur. J. Cancer* **2012**, *48*, 1682−1691.
(22) Huang, D.; Peng, X.; Su, L.; Wang, D.; Khuri, F. R.; Shin, D. M.; Chen, Z. G. *Nano Res.* **2010**, *3*, 61−68.
(23) Shi, C.; Zhou, G.; Zhu, Y.; Su, Y.; Cheng, T.; Zhau, H. E.; Chung, L. W. K. *Eur. J. Histochem.* **2008**, *52*, 127−134.
(24) Liu, J.; Lau, S. K.; Varma, V. A.; Moffitt, R. A.; Caldwell, M.; Liu, T.; Young, A. N.; Petros, J. A.; Osunkoya, A. O.; Krogstad, T.; Leyland-Jones, B.; Wang, M. D.; Nie, S. *ACS Nano* **2010**, *4*, 2755−2765.
(25) Chen, C.; Peng, J.; Xia, H.; Yang, G.; Wu, Q.; Chen, L.; Zeng, L.; Zhang, Z.; Pang, D.; Li, Y. *Biomaterials* **2009**, *30*, 2912−2918.
(26) Mattoussi, H.; Mauro, J. .; Goldman, E. R.; Anderson, G. P.; Sundar, V. C.; Mikulec, F. V.; Bawendi, M. G. *J. Am. Chem. Soc.* **2000**, *122*, 12142−12150.
(27) Goldman, E. R.; Anderson, G. P.; Tran, P. T.; Mattoussi, H.; Charles, P. T.; Mauro, J. M. *Anal. Chem.* **2002**, *74*, 841−847.
(28) Goldman, E. R.; Medintz, I. L.; Hayhurst, A.; Anderson, G. P.; Mauro, J. M.; Iverson, B. L.; Georgiou, G.; Mattoussi, H. *Anal. Chim. Acta* **2005**, *534*, 63−67.